Various Forms of Stress Corrosion in AISI 316 Austenitic Stainless Steel

B. BREVAGLIERI, M. MONGELLI, S. NATALI. Dip. Chemical Engineering, Materials, Raw Materials and Metallurgy. - Università "La Sapienza" Roma.

Abstract

A heat-treated AISI 316 austenitic stainless steel has been studied in H_2SO_4+NaCl test solutions with various SO_4=/Cl^- ratios, namely 2.5/0.5, 1/0.2, 2.5/0.2, 1/0.5 (all concentrations expressed in normality), at constant load and at room temperature.
The SEM examination has been used to ascertain the morphology and evolution of attack, initiated at preformed pits having critical dimensions, owing to the fact of polarization in the imperfect passivity zone and subsequently, alternatively in the regions of perfect passivity, active passive transitions, activity and in freely corroding conditions.
Reverse and direct polarization sequences have been investigated. It has been observed that in some cases the intergranular attack changes to transgranular, in other cases the transgranular attack changes to intergranular. It has been confirmed that the AISI 316 stainless steel is sensitive to the intergranular attack.

Riassunto

E' stato studiato un acciaio inossidabile austenitico AISI 316 nello stato solubilizzato sotto un carico costante pari all'80% σp, a temperatura ambiente ed in soluzioni di prova costituite da H_2SO_4+NaCl con vari rapporti $S0_4$=/Cl-: 2.5/0.5, 1/0.2, 2.5/0.2, 1/0.5 (concentrazioni espresse in normalità).

Mediante osservazioni al microscopio a scansione è stata studiata la morfologia e l'evoluzione dell'attacco, innescato in corrispondenza di cavità preformate con dimensioni critiche, per effetto della polarizzazione nella zona di passività imperfetta e successivamente in alternativa fra loro, nelle regioni di passività perfetta, di transizione attivo-passiva, di attività e di libera corrosione. Sono state sperimentate sequenze di polarizzazione inverse, oltre che dirette.

E' stato osservato che in alcuni casi l'andamento intergranulare dell'attacco si modifica in transgranulare, in altri casi viceversa. E' confermata la sensibilità degli acciai inossidabili AISI 316 alla corrosione intergranulare.

Introduction

It is generally accepted that the AISI 316 stainless steel is less sensitive to stress corrosion than AISI 304 stainless steel [1]. The main reason of this difference is that AISI 316 stainless steel contains more nickel and molybdenum, this causes an oxide film that is more resistent to stress corrosion in chlorinated water. The austenitic matrix of AISI 316 is also more stable than that of AISI 304 stainless steel, because the latter can be more easily transformed to martensite [1].

Nevertheless, it has been showed that AISI 316 stainless steel is sensitive to intergranular attack in some ranges of potential [2], in fact, for high contents of oxygen, noble electrochemical potentials are generated and they produce stress corrosion cracking.

The object of this paper is to find the ranges of potential where stress corrosion cracking occurs. Stainless steels are usually exposed in environments where they are in the passivity zone. In the industrial practice, stress corrosion stars when pitting and crevice corrosion are active, since the pits and crevices act as stress raisers that favour crack nucleation.

These considerations justify the study of the effect of preformed pits on the corrosion behaviour of an AISI 316 austenitic stainless steels.

The samples were stressed by a constant tensile load equal to 80 % $\sigma_{p(02)}$. Experiments were conducted within the following potential ranges: imperfect passivity region, active-passive region, active region. The environment was characterized by the presence of passivating and depassivating species.
Moreover, SEM examination has been used to ascertain morphology and evolution of the attack on samples containing intergranular microcracks produced by polarization in the imperfect passivity region, and subsequently polarized in the regions of active-passive transitions and "vice-versa".

Materials and Equipment

The experiments were run on a rod of AISI 316 austenitic stainless steel of 10 mm in diameter whose composition (% wt.) is: C = 0.06; Cr = 17; Ni =12, Mn = 1; Mo = 2-3; S and P are completely absent.

From the rod tensile test specimens 40 mm long and 4 mm in diameter have been produced. After machining, the specimens were heat treated at 1050°C and water quenched;the oxide layer and the chromium depleted steel layer were then removed by emery paper, and the final surface finish was carried out using wet SiC 1000 paper.

H_2S0_4 + NaCl test solutions were prepared with various SO_2=/CI^- ratios, namely 2.5/0.5, 1/0.2, 2.5/0.2, 1/0.5 (all concentrations are expressed in terms of normality). The chosen solutions where those with 1/0.2 and 2.5/0.5 ratios, because they were found to be the best solutions in order to investigate the stress corrosion: the other solutions gave generalized corrosion or other forms of non localized attack. The solutions were thermostatated at room temperature.

In the electrochemical tests, the cell consisted of a cylindrical Pyrex container closed with a neoprene stopper through which the specimen was passed. The cell also contained a platinum-wire counter-electrode and a Luggin capillary connected to a saturated calomel electrode (SCE). The electrochemical tests were performed with an AMEL Corrograph model 561 B. The specimens were examined under a Hitachi S2500 scanning electron microscope (SEM).

Experimental Results

The samples were polarized at potentials more noble than E_R (breakdown potential) to obtain several pits with critical dimensions (stage 1), as shown in the cyclic polarization curve of fig. 1 [4]

This phase is common to all the tests of this work, because it has been found [5,6,7] that stress corrosion starts when pitting and crevice corrosion are active, since the pits and crevices act as stress raisers that enable the nucleation of cracks.

The perfect passivity potential E_ρ, the imperfect passivity potential E_p and the primary passive potential $E_{\rho\rho}$ have been found on the cyclic polarization curves. The imperfect passivity zone (E_R - E_ρ) (stage 2), the passivity zone (E_ρ - E_p) (stage 3), the active-passive zone (E_p - $E_{\rho\rho}$) (stage 4), and the active zone (stage 5) were also defined.

Using solutions having a SO_4^{--}/Cl^- ratio of 1/0.2, the imperfect passivity interval lies between 300 and 850 mV.

The specimens, under a constant tensile load equal to 80 % $\sigma_{p(02)}$ (200 N/mm^2), polarized at a potential between 710 and 830 mV, in the upper part of the Imperfect passivity zone (stage 2) [8], after an exposure of 95 h, show intergranular attack on the bottom of the preformed pits (Fig. 2). With the same SO_4^{--}/Cl^- ratio, but at a potential of-150 mV (active-passive zone) (stage 4), after an exposure of 20 h, the specimens show intergranular attack inside as well as outside the pits (Fig. 3); in the active zone (stage 5) at -285 mV, no localised corrosion can be observed, except for very small cracks.

Using the 2.5/0.5 ratio, the imperfect passivity interval is the same as the one obtained using the 1/0.2 ratio.

At potential between 800 and 830 mV, in the upper part of the imperfect passivity zone, after an exposure of 21 h only, a strikingly localised corrosion of caving pits, covered with a thin metallic layer and full of flake metal residues is present.

The still covered cavities can be barely seen in Fig. 4a, while in Fig. 4b those cavities have been partly broken through.

The morphology of the phenomenon resembles that observed in the initial step of stress corrosion of sensitized austenitic stainless steels [9].

In order to avoid this phenomenon, which can not be considered stress corrosion, potentials between 710 and 800 mV, in the lower part of the imperfect passivity zone have been used, too. After an exposure of 95 h, intergranular attack on the bottom of pits can be observed Fig. 5

At active-passive potentials, (stage 4) (-150 mV), the intergranular attack on the whole specimen appears Fig. 6. In the active zone (stage 5), the transgranular attack appears Fig. 7, microcracks are present on the preformed pits, and the crack walls reveal corrosion of the fine parallel pleat type, which is typical of transgranular corrosion.

Table 1 summarizes the above mentioned experimental data.

TABLE 1 - Experimental conditions

SOLUTION	STAGE	DURATION	POTENTIAL	TYPE OF CORROSION
1/0.2	2	42h	780 mV	INTERGRANULAR
1/0.2	2	72h	800 mV	INTERGRANULAR
1/0.2	2	95h	830 mV	INTERGRANULAR
2.5/0.5	2	42h	830 mV	CAVITIES
2.5/0.5	2	21h	830 mV	CAVITIES
2.5/0.5	2	95h	710 mV	INTERGRANULAR
2.5/0.5	2	93h	730 mV	INTERGRANULAR
2.5/0.5	2	100h	710 mV	INTERGRANULAR
1/0.2	3	30h	150 mV	NO STRESS CORROSION
1/0.2	3	48h	170 mV	NO STRESS CORROSION
2.5/0.5	3	30h	150 mV	NO STRESS CORROSION
2.5/0.5	3	48h	150 mV	NO STRESS CORROSION
1/0.2	4	20h	-150 mV	INTERGRANULAR
1/0.2	4	42h	-135 mV	INTERGRANULAR
1/0.2	4	48h	-135 mV	INTERGRANULAR
2.5/0.5	4	20h	-150 mV	INTERGRANULAR
2.5/0.5	4	25h	-150 mV	INTERGRANULAR
2.5/0.5	4	30h	-150 mV	INTERGRANULAR
1/0.2	5	25h	-285 mV	NO STRESS CORROSION
1/0.2	5	42h	-290 mV	NO STRESS CORROSION
2.5/0.5	5	40h	-290 mV	INTERGRANULAR
2.5/0.5	5	36h	-285 mV	INTERGRANULAR
2.5/0.5	5	42h	-290 mV	INTERGRANULAR

Other experiments have been carried out on the specimens, operating a combination of the above men-

tioned stages. The 2.5/0.5 ratio, which is the most sensitive to stress corrosion, has been used. The chosen combinations are 1-2-5, 1-5-2, 1-4-5 and 1-5-4.

In the experimental results concerning the combination 1-2-5, the specimen shows, on the bottom of the preformed pits, intergranular and transgranular attack. The combination 1-4-5 shows a similar result, but less evident.

The reverse combinations, 1-5-2 and 1-5-4, give results like the direct combinations Figs. 8 and 9. Table 2 summarizes the above mentioned results.

Table 2 - Experimental conditions

COMBINATION	STAGE	DURATION	POTENTIAL	STAGE	DURATION	POTENTIAL	TYPE OF CORROSION
125	2	93 h	730 mV	5	36 h	-285 mV	INTER. + TRANS.
125	2	96 h	750 mV	5	42 h	-290 mV	INTER. + TRANS.
125	2	96 h	780 mV	5	46 h	-285 mV	INTER. + TRANS.
152	5	36 h	-285 mV	2	96 h	730 mV	TRANS. + INTER.
152	5	42 h	-290 mV	2	96 h	750 mV	TRANS. + INTER.
152	5	46 h	-290 mV	2	96 h	780 mV	TRANS. + INTER.
145	4	25 h	-150 mV	5	40 h	-285 mV	TRANS. + INTER.
145	4	30 h	-150 mV	5	42 h	-290 mV	INTER. + TRANS.
145	4	30 h	-150 mV	5	40 h	-290 mV	INTER. + TRANS.
154	5	40 h	-290 mV	4	25 h	-150 mV	TRANS. + INTER.
154	5	42 h	-290 mV	4	30 h	-150 mV	TRANS. + INTER.
154	5	42 h	-290 mV	4	25 h	-150 mV	TRANS. + INTER.

Discussion

The stress corrosion occurs when the formation rate and the dissolution rate of slip steps are comparable. The formation rate of the slip steps depends on the dynamic strain rate and on the stress applied in the constant load test, while the dissolution rate of slip steps depends on the corrosiviteness of the environment [1]. When the formation rate of the slip steps is greater than their dissolution rate, the formation of the steps can be observed, and their dissolution becomes the controlling stage of the whole process [10], [11], [12]; then, the transgranular attack is observed.

The intergranular attack occurs when, in easy passivation conditions (from the point of view of kinetics), dislocations move and thicken on the grain boundaries, creating a larger number of active zones, also because of an increase in the number of stress raisers.

Keeping the applied load constant, as well as the formation rate of the slip steps, the attitude of steel to passivate can be modified, by means of potential variations. Thus, dissolution rates greater or smaller than the formation rates of the slip steps can be obtained.

By varying the applied load and potential, as previously found by us [5] and other scientists[13], the two different forms of stress corrosion can be established; otherwise, the stress corrosion degenerates into other forms of attack such as pitting corrosion, sometimes causing very deep cavities or tunnels, or generalized corrosion.

Using a 2.5/0.5 ratio, intergranular corrosion on the bottom of cavities (in the perfect passivity zone) and on the whole specimen (in the active-passive zone) has been observed.

This case can be described in terms of "easy passivation condition (from the point of view of kinetics)", as previously defined.

In the active zone, the transgranular attack occurs; in fact, by keeping constant the tensile load as well as the strain rate of the slip steps, it will always be greater than the easy passivation one.

At a potential between 800 and 830 mV a strikingly localised corrosion of caving pits can be observed. In this case, the dissolution rate of the slip steps and the passivation rate are not comparable, and the stress corrosion occurs with very deep cavities.

In this case, the corrosion shows as a pitting corrosion, instead of a stress corrosion.

From the experimental results of the combinations 1-2-5 and 1-4-5, the intergranular attack and the transgranular attack can be observed. Anyway, it must be noted, that they do not occur at the same time, because the latter occurs before the former.

More precisely, the transgranular behaviour of the cracks, which is a distinctive effect of the active zone polarization, stage 5, starts at the boundary of the grains which have been attacked in the previous stages 2 and 4, when the experimental conditions enter the active zone.

Examining the corrosion results of reverse sequences 1-5-2 and 1-5-4, the intergranular and transgranular attack, like the previous cases, can be observed.

The active initial conditions, thus, do not prevent the intergranular corrosion, as found for the AISI 304 austenitic stainless steel.

Thus, the sensitivity of AISI 316 stainless steel to intergranulation corrosion is confirmed.

Conclusions

Various kinds of stress corrosion forms can be produced in an austenitic stainless steel, depending on the conditions to which it is subjected. It has been varied the rate of attack of the slip steps, formed as a result of the loads applied by polarizing in different regions and it has been obtained typical morphologies of stress corrosion.

This methodology is usefull for identifying and reproducing the real phenomena under different experimental conditions, with satisfactory reproducibility, in a relatively brief space of time.

References

[1] J. Congleton, W. Zheng, H. Hua, *Corrosion Science*, 30, (6/7), 555-567, 1990.
[2] A.H. Advani, L.E. Murr, D.G. Atteridge, R. Chelakara, S.M. Bruemmer, *Corrosion*, 47, (12), 939-952,1991.
[3] R. Nishimura, K.Kudo, *Corrosion*, 45, (4), 308-316,1989.
[4] R. Nishimura, K. Kudo, *Corrosion Science*, 31, 479-484, 1990.
[5] A. Alderisio, B. Brevaglieri, G. Signorelli, *Metall.Sci. Technol.*, 7, (1), 76-83, 1989.
[6] R.N. Parkins, *Met.Technol.*, 9, 122-129, 1982.
[7] G. Cragnolino, L.F. Lin, Z. Szklarska-Smialowska, *Corrosion*, 37, (6), 312-320,1981.
[8] J. Congleton, W. Zeng, H. Hua, *Corrosion*, 46, (8), 621-627,1990.
[9l H.E. Hanninen, *International Metals Reviews*, (3), 85-133,1979.
[10] M. Takano, *Corrosion*, 30, (12), 441446,1979.
[11] H. Okada, Y. Hosoy, S. Abe, Corrosion, 27, (10), 424-428,1971.
[12] T. Nakayama, M. Takano, *Corrosion*, 38, (1), 1-9, 1982.
[13] G.S. Duffo', I.A. Mayer, J.R. Galvele, *Corrosion Science*, 28, (10), 1003-1018, 1988.

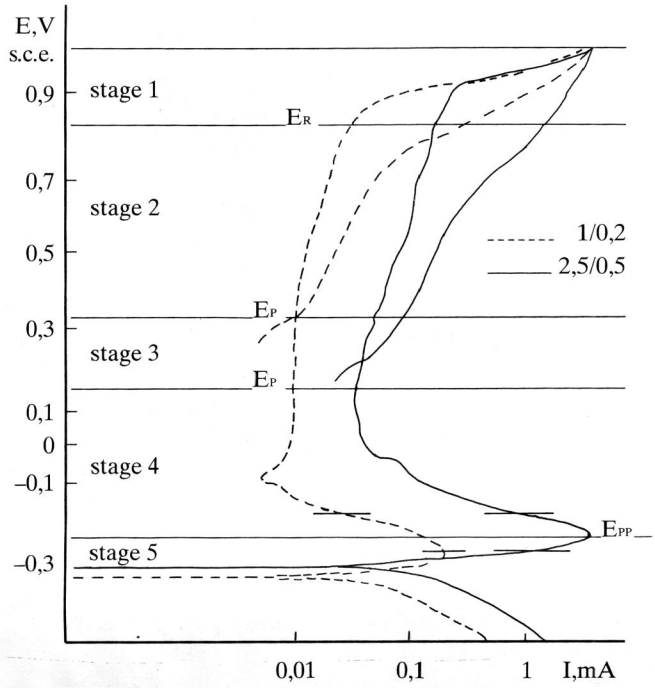

Fig. 1
Cyclic polarization curve in 1N H_2SO_4+NaCl and 2.5N H_2SO_4+0,5N NaCl

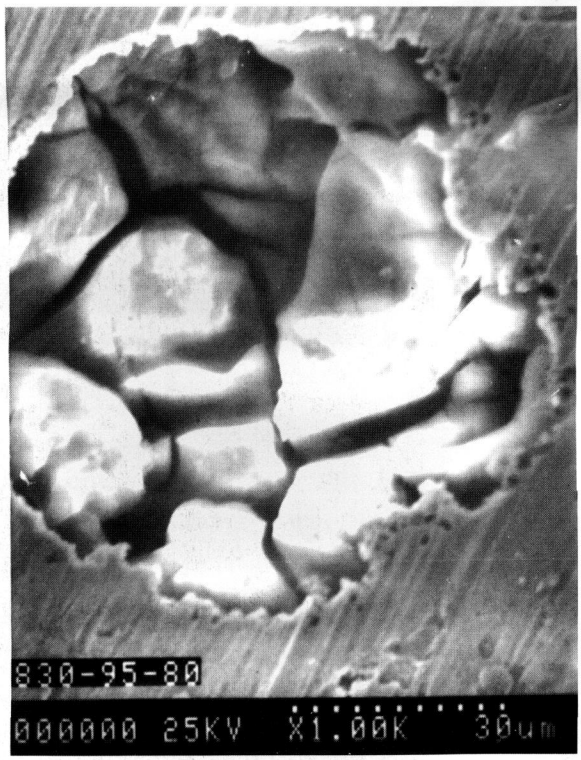

Fig. 2
Intergranular attack on bottom of preformed pit. (stage 2: 830 mV, 95h, 1/0,2) x 1000

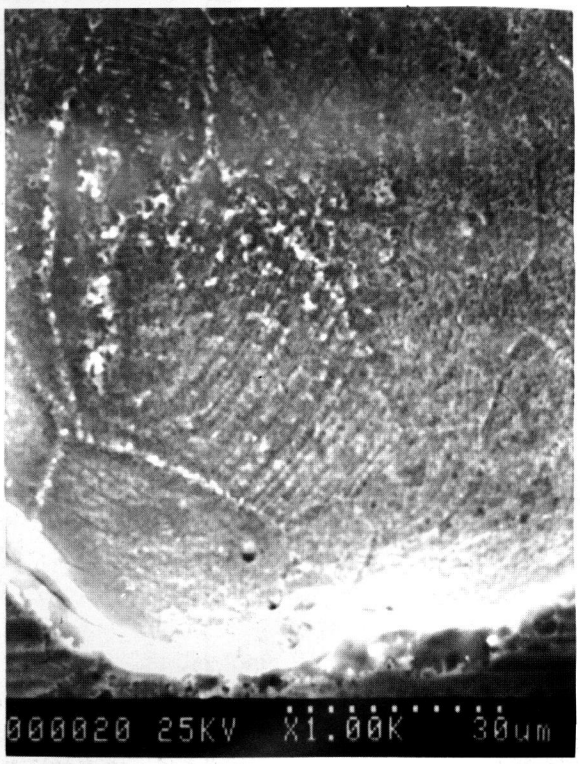

Fig. 3
Light intergranular attack.
(stage 3: 150 mV, 20h, 1/0,2) x 1000

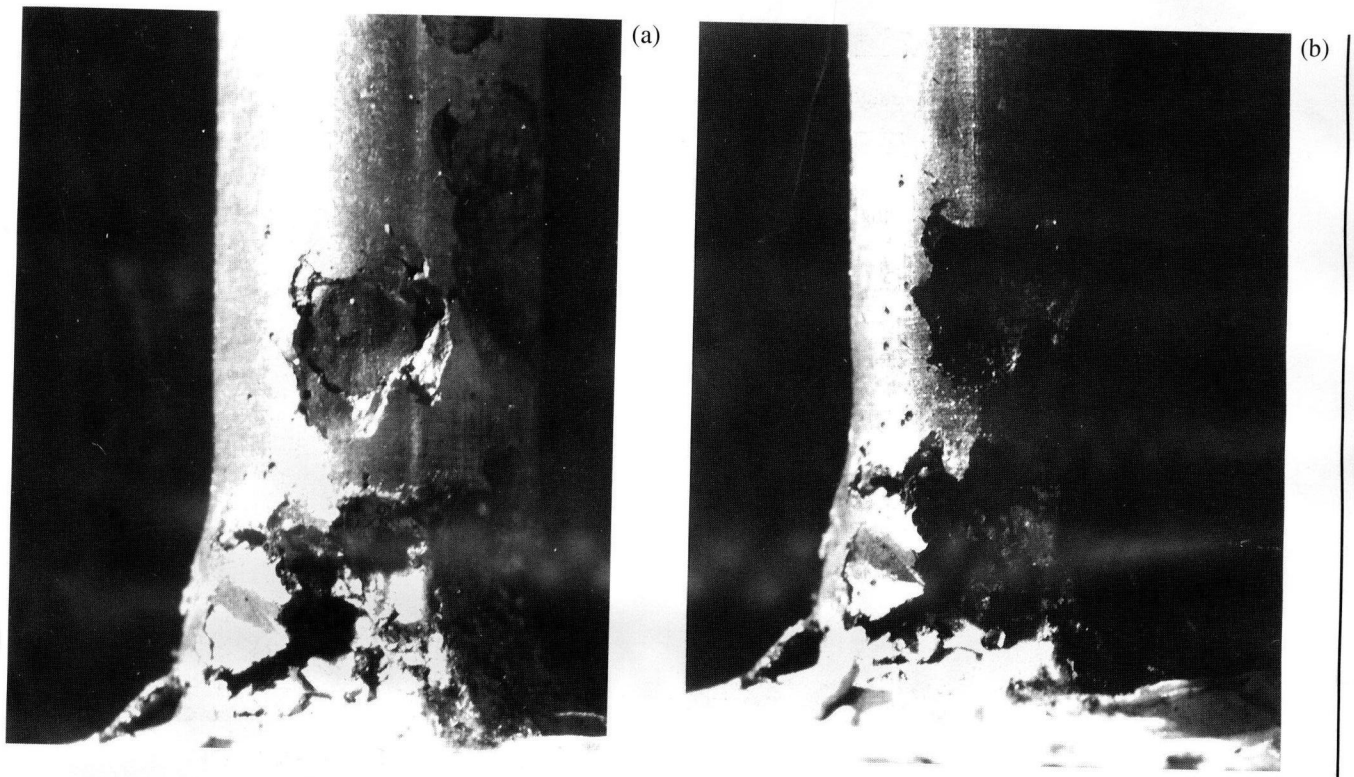

Fig. 4
(a) Cavities covered with a thin metallic layer (stage 2: 830 mV, 42h, 2,5/0,5) x 12
(b) partially broken cavities (stage 2: 830 mV, 42h, 2,5/0,5) x 12

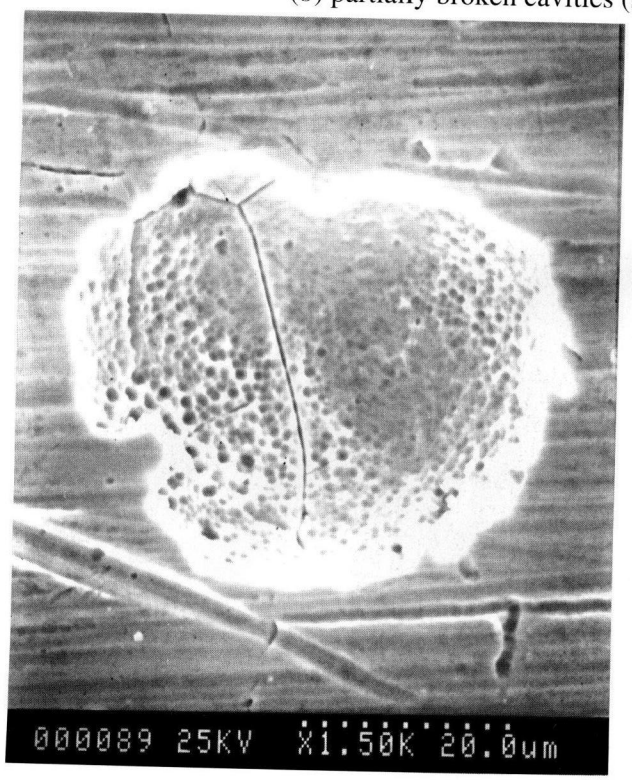

Fig. 5
Intergranular attack on bottom preformed pit (stage 2: 710 mV, 95h, 2,5/0,5) x 1500

Fig. 6
Intergranular attack on the whole surface.
(stage 4: -150 mV, 20h, 2,5/0,5) x 2000

Fig. 7
Transgranular attack with barely marked fine parallel pleat pattern.
(stage 5: -290 mV, 42h, 2,5/0,5) x 1500

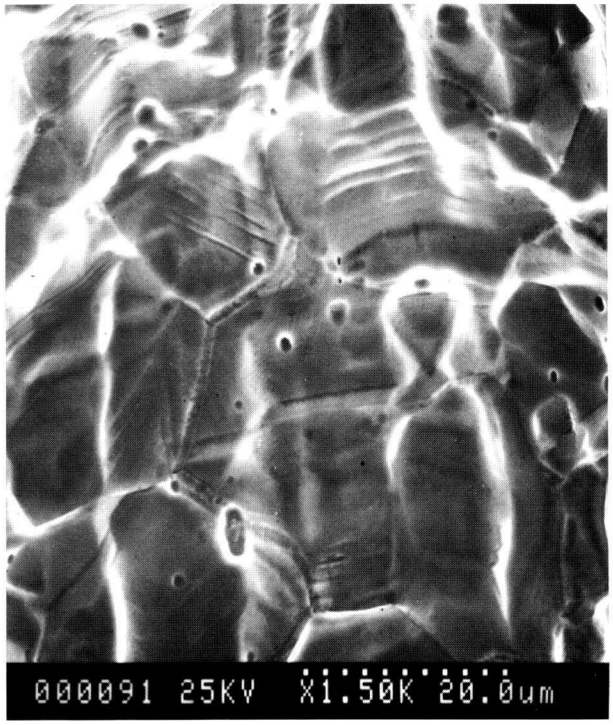

Fig. 8
Intergranular and transgranular attack .
(stage 5: -290 mV, 96h, 2,5/0,5) +
(stage 2: 780 mV, 46h, 2,5/0,5) x 1500

Fig. 9
Intergranular and transgranular attack . (stage 5: -290 mV, 42h, 2,5/0,5) +
(stage 4: -150 mV, 30h, 2,5/0,5) x 1500